

## Supplementary Information

### Effects of dissolved organic matter characteristics on the photosensitized degradation of pharmaceuticals in wastewater treatment wetlands

Arpit Sardana<sup>a,b\*</sup>, Leah Weaver<sup>a</sup>, Tarek N. Aziz<sup>a</sup>

<sup>a</sup>Department of Civil, Construction, and Environmental Engineering, North Carolina State University  
3250 Fitts-Woolard Hall, 915 Partners Way, Raleigh NC 27695, USA

<sup>b</sup>Geosyntec Consultants Inc.,  
2501 Blue Ridge Road, Suite 430, Raleigh, NC, 27607, USA

\*Corresponding author email address: [asardan@alumni.ncsu.edu](mailto:asardan@alumni.ncsu.edu)

*Submitted to Environmental Science: Process and Impacts*

## Table of Contents

Section S1: Sampling Locations .....	3
Section S2: Chemicals .....	4
Section S3: Properties of target pharmaceuticals.....	5
Section S4: HPLC methods .....	7
Section S5: Photochemical modelling .....	8
Section S6: Water chemistry.....	9
Section S7: DOM polarity assessment.....	10
Section S8: Photodegradation kinetics.....	11
Section S9: Steady state concentration estimates.....	13
Section S10: Amoxicillin degradation in the dark controls .....	14
Section S11: Noteworthy correlations .....	15
Section S12: References .....	18

## Section S1: Sampling Locations

Table S1: List of sampling locations, sample IDs, and process categories for the two sites.

Samples were collected from the Walnut Cove treatment wetland site in September 2018 and the five samples from the Neuse River Resource Recovery Facility were collected in November 2019. All locations from the sites were sampled on the same day. The sampling locations are listed in the sequence of treatment processes.

<b>Walnut Cove wastewater treatment wetland site</b>	
<i>Sampling location (11 samples)</i>	<i>Process category</i>
DBR - distribution box raw sewage	sewage
WWL - wastewater lagoon	lagoon treated wastewater
SAP - second aeration pond	“
SPI - serpentine pond inlet	“
SPM - serpentine ponds midpoint	“
DBC - distribution box cattail cells	“
ICM - inner cattails midpoint	vegetated wetland cells
OCM - outer cattail cell outlet midpoint	“
ICO - inner cattail cell outlet	“
OCO - outer cattail cell outlet	“
TFD - Town Fork creek downstream	downstream discharge
<b>Neuse River Resource Recovery Facility (NRRRF, Raleigh, NC)</b>	
<i>Sampling location (5 samples)</i>	<i>Process category</i>
NRRRF 1 - post screening and grit removal	WWTP primary effluent
NRRRF 2 - post primary clarifier (before biological nutrient removal (BNR) basins)	“
NRRRF 3 – middle of BNR basin	WWTP secondary effluent
NRRRF 4 - post BNR denitrification (pre-denitrification beds)	“
NRRRF 5 - post denitrification beds (pre-UV treatment)	“

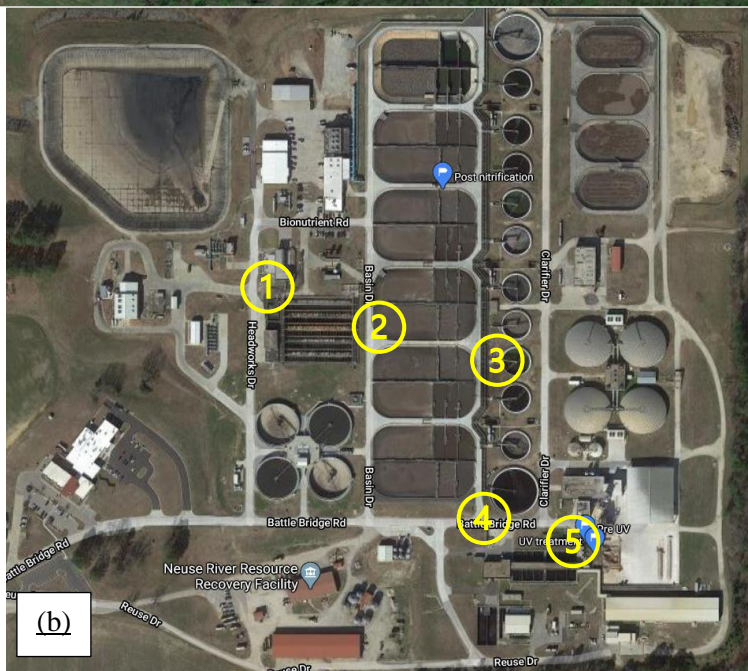


Figure S1: The aerial images of the two sampling sites - a) treatment wetland site at Walnut Cove, NC and b) Neuse River Resource Recovery Facility (NRRRF), Raleigh, NC. Refer to Table S1 for details about process and sampling locations.

## Section S2: Chemicals

HPLC grade organic solvents such as methanol, acetonitrile, and isopropyl alcohol were purchased from Fisher Scientific. All solutions and mobile phase were prepared using high purity water ( $> 18 \text{ M}\Omega$ ). Atenolol (98%),  $17\alpha$ -ethinylestradiol (98%), and p-nitroanisole (99%) were purchased from ACROS Organics. Cimetidine (98%) was purchased from Alfa Aesar. Amoxicillin (potency  $\geq 900 \mu\text{g per mg}$ ) was purchased from Sigma Aldrich. ACS grade pyridine was purchased from Fisher Scientific. All other chemicals used were ACS grade or better.

## Section S3: Properties of target pharmaceuticals

Table S2: Structure and properties of the target pharmaceuticals.

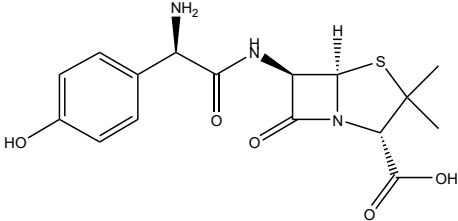
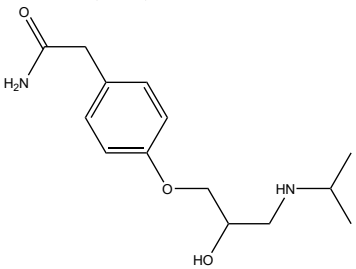
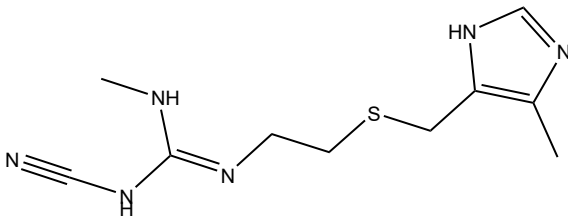
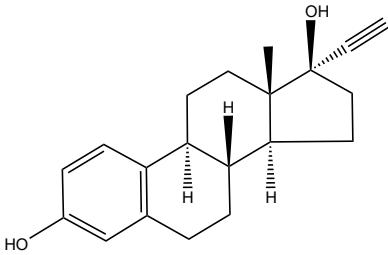
Structure	Solubility in water	pKa	log Kow	References
<p>Amoxicillin (AMX)</p> 	400 mg L <sup>-1</sup>	2.7, 7.5, 9.6	0.87	(Yoon et al., 2004), (Cass et al., 2003)
<p>Atenolol (ATL)</p> 	Soluble	9.6	0.16	(Liu and Williams, 2007), (Küster et al., 2007)
<p>Cimetidine (CME)</p> 	freely soluble	7.1	0.57	(Latch et al., 2003), (Zenobio et al., 2015)
<p>17<math>\alpha</math>-ethinylestradiol (EE2)</p> 	4.8 mg L <sup>-1</sup>	10.5	3.67	(Ren et al., 2016)

Table S3: Biomolecular rate constants  $k_{P,PPRI}$  ( $M^{-1} s^{-1}$ ) and direct photolysis quantum yields (unitless) for the target pharmaceuticals from previous studies.

Target pharmaceutical (P)	Direct photolysis quantum yield ( $\Phi$ )	$k_{P,^1O_2}$	$k_{P,\cdot OH}$	$k_{P,CO_3^-}$
AMX	$5.97 \times 10^{-3}$ at pH 7.5, $4.47 \times 10^{-3}$ at pH 5.5 (Andreozzi et al., 2004)	$1.44 \times 10^4$ (Xu et al., 2011)	$6.94 \times 10^9$ (Song et al., 2008a)	-
ATL	$1.1 \times 10^{-2}$ (Yamamoto et al., 2009)	$8.5 \times 10^3$ (Wang et al., 2012)	$7.5 \times 10^9$ (Benner et al., 2008; Song et al., 2008b)	$(9 \pm 4) \times 10^6$ for protonated; $(5.9 \pm 1.6) \times 10^7$ for deprotonated (Jasper and Sedlak, 2013)
CME	-	$(9.2 \pm 0.6) \times 10^7$ for pH 6.9; $(0.33 \pm 0.03) \times 10^7$ for pH 4.2, protonated; $(25 \pm 2) \times 10^7$ for pH 10.2, deprotonated (Latch et al., 2003)	$(650 \pm 50) \times 10^7$ for pH 3 (Latch et al., 2003)	-
EE2	0.01 (Ren et al., 2016)	$9.71 \times 10^7$ (Ren et al., 2016)	$1.09 \times 10^{10}$ (Ren et al., 2016), $(9.8 \pm 1.2) \times 10^{10}$ (Huber et al., 2003)	-

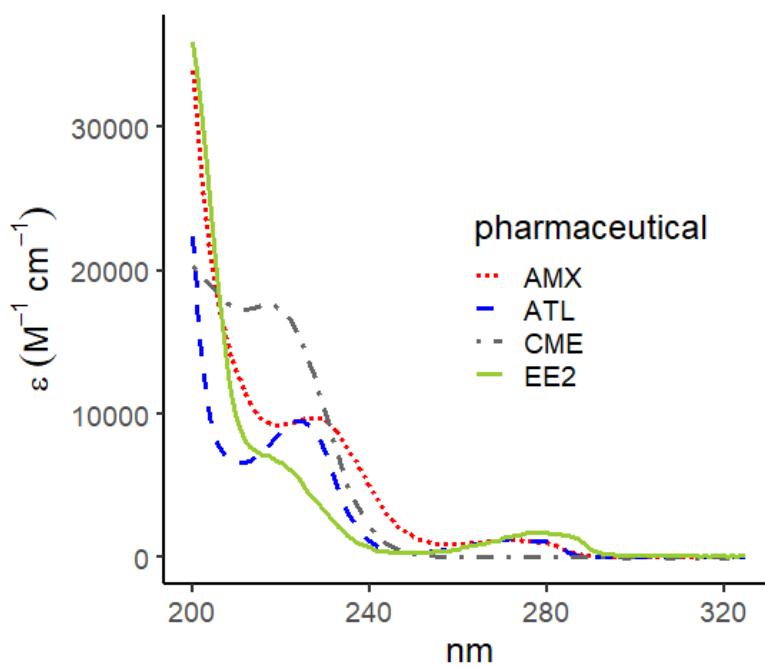


Figure S2: Molar absorption spectra of the target pharmaceuticals.

## Section S4: HPLC methods

Table S4: HPLC methods for measurement of pharmaceuticals, actinometry, and UV characterization of DOM.

Detection	Stock solution preparation	Initial concentration	Irradiation duration	Column	Isocratic mobile phase (1 ml min <sup>-1</sup> )	Detection wavelength
AMX	500 mg L <sup>-1</sup> in KH <sub>2</sub> PO <sub>4</sub> buffer (10mM, pH 7)	15 mg L <sup>-1</sup>	10 h	Phenomenex Gemini C18 (250 x 4.60 mm, 5 µm particles)	15% methanol:85% KH <sub>2</sub> PO <sub>4</sub> buffer (10mM, pH 3)	230 nm
ATL	500 mg L <sup>-1</sup> in HPLC grade water	20 mg L <sup>-1</sup>	5 h	Agilent XDB C18 (150 x 4.60 mm, 5 µm particles)	10% methanol:90% KH <sub>2</sub> PO <sub>4</sub> buffer (10mM, pH 3)	224 nm
CME	1000 mg L <sup>-1</sup> in HPLC grade water	20 µM	1.5 h	Agilent XDB C18 (150 x 4.60 mm, 5 µm particles)	10% methanol:90% KH <sub>2</sub> PO <sub>4</sub> buffer (10mM, pH 3)	218 nm
EE2	1000 mg L <sup>-1</sup> in acetonitrile (100%)	3.75 mg L <sup>-1</sup>	6 h	Phenomenex Gemini C18 (250 x 4.60 mm, 5 µm particles)	60% acetonitrile:40% Water (0.1% acetic acid)	280 nm
actinometry analyte, p-nitroanisole (PNA)	10 mM PNA in 100% ACN, 50 mM pyridine in pure water	10 µM PNA in 5.5 mM pyridine	1.25 h	Agilent XDB C18 (150 x 4.60 mm, 5 µm particles)	60% acetonitrile:40% Water (0.1% acetic acid)	313 nm
UV detection of DOM	-	-	-	Agilent XDB C18 (150 x 4.60 mm, 5 µm particles)	10% methanol:90% KH <sub>2</sub> PO <sub>4</sub> buffer (10mM, pH 3)	224 nm

## Section S5: Photochemical modelling

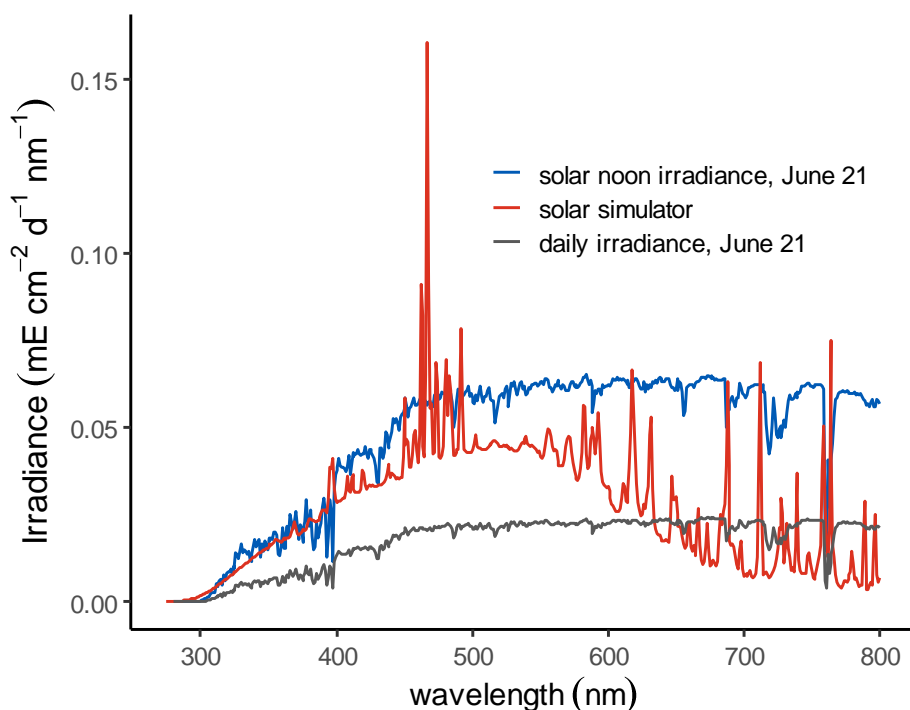


Figure S3: Irradiance spectra of the solar simulator. The estimate daily and solar noon irradiance for June 21 at 40° N latitude from Apell and McNeill, 2019 are also shown.

### Rate of light absorption and screening factors

The total rate of light absorption by sample DOM was calculated over 275-650 nm using the lamp spectral irradiance,  $I_\lambda$ , from PNA-pyr actinometry (Eq. S1).  $a_\lambda$  ( $\text{m}^{-1}$ ) is the decadic absorbance of irradiated samples and  $z$  is the effective path length (m) of the quartz test tubes used during experiments. Light screening factors ( $S_{\text{pharma, DOM}}$ ) for target pharmaceuticals were calculated as the ratio of light absorbed in the presence and absence of sample DOM (Ekrem Karpuzcu et al., 2016; Langlois et al., 2014). Equations S3 to S5 detail the calculations involved in determining wavelength specific light rate of light absorption for individual components (i and j) of a solution of dissolved pharmaceutical in sample DOM. Direct photolysis rates were multiplied with screening factors to estimate direct photodegradation rates in DOM samples.

$$R_a = \sum_{\lambda=275 \text{ nm}}^{650 \text{ nm}} I_\lambda (1 - 10^{-a_\lambda z}) \quad \text{Eq. S1}$$

$$R_{a,i_\lambda} = I_\lambda (1 - 10^{-a_{i_\lambda} l}) \quad \text{Eq. S2}$$

$$R_{a,i\_j\lambda} = I_\lambda \left( 1 - 10^{-(a_{i_\lambda} + a_{j_\lambda}) l} \right) \frac{a_{i_\lambda}}{a_{i_\lambda} + a_{j_\lambda}} \quad \text{Eq. S3}$$

$$S_{i,j} = \frac{\int_{\lambda_{\text{low}}}^{\lambda_{\text{high}}} R_{a,i\_j\lambda}}{\int_{\lambda_{\text{low}}}^{\lambda_{\text{high}}} R_{a,i_\lambda}} \quad \text{Eq. S4}$$



## Section S6: Water chemistry

Table S5: Water chemistry measurements and optical properties from UV-Vis and EEM measurements for filtered DOM samples. Average and standard deviation ( $\pm$  s.d) are presented.

variable (units)	Walnut Cove wetland site				NRRRF	
	Sewage (n = 1)	lagoon treated wastewater (n = 5)	vegetated wetland cells (n = 4)	downstream discharge (n = 1)	WWTP primary effluent (n = 2)	WWTP secondary effluent (n = 3)
DOC (mg L <sup>-1</sup> )	6.28	9.84 $\pm$ 0.74	8.96 $\pm$ 1.00	4.06	25.60 $\pm$ 0.30	7.14 $\pm$ 0.21
Fe (mg L <sup>-1</sup> )	0.18	0.64 $\pm$ 0.44	0.46 $\pm$ 0.32	0.49	0.33 $\pm$ 0.22	0.09 $\pm$ 0.05
R <sub>s</sub> (mol-photons L <sup>-1</sup> s <sup>-1</sup> )	7.00E-06	8.75E-06 $\pm$ 5.54E-06	6.96E-06 $\pm$ 2.33E-06	2.95E-06	1.22E-05 $\pm$ 1.74E-06	4.20E-06 $\pm$ 7.95E-08
BIX	0.92	0.87 $\pm$ 0.04	0.84 $\pm$ 0.02	0.75	0.91 $\pm$ 0.12	0.82 $\pm$ 0.05
B peak (R.U.)	1.75	1.64 $\pm$ 0.49	1.45 $\pm$ 0.66	0.34	2.69 $\pm$ 0.71	0.90 $\pm$ 0.02
T peak (R.U.)	2.21	1.77 $\pm$ 0.62	1.58 $\pm$ 0.75	0.34	3.68 $\pm$ 0.96	1.24 $\pm$ 0.02
A peak (R.U.)	1.55	2.38 $\pm$ 0.18	2.53 $\pm$ 0.13	1.23	2.80 $\pm$ 0.26	2.49 $\pm$ 0.10
M peak (R.U.)	1.26	1.69 $\pm$ 0.15	1.78 $\pm$ 0.11	0.81	2.38 $\pm$ 0.25	2.12 $\pm$ 0.10
C peak (R.U.)	1.48	1.51 $\pm$ 0.11	1.55 $\pm$ 0.07	0.69	2.29 $\pm$ 0.05	2.61 $\pm$ 0.32
Peak C : T	0.67	0.94 $\pm$ 0.33	1.12 $\pm$ 0.41	2.05	0.64 $\pm$ 0.15	2.10 $\pm$ 0.28
Peak A : T	0.70	1.48 $\pm$ 0.53	1.83 $\pm$ 0.70	3.63	0.78 $\pm$ 0.13	2.01 $\pm$ 0.10
Peak C : A	0.95	0.64 $\pm$ 0.03	0.61 $\pm$ 0.02	0.57	0.82 $\pm$ 0.06	1.04 $\pm$ 0.09
FI	1.79	1.56 $\pm$ 0.05	1.49 $\pm$ 0.02	1.38	1.70 $\pm$ 0.03	1.81 $\pm$ 0.06
HIX	0.61	0.72 $\pm$ 0.05	0.75 $\pm$ 0.06	0.84	0.63 $\pm$ 0.04	0.80 $\pm$ 0.00
a <sub>254</sub> (Napierian m <sup>-1</sup> )	45.15	75.18 $\pm$ 28.83	68.98 $\pm$ 11.40	36.90	80.52 $\pm$ 6.62	41.43 $\pm$ 0.66
a <sub>300</sub> (Napierian m <sup>-1</sup> )	27.14	44.72 $\pm$ 19.58	40.16 $\pm$ 7.41	22.19	48.18 $\pm$ 3.03	24.90 $\pm$ 0.71
E2:E3	3.39	4.47 $\pm$ 0.48	4.67 $\pm$ 0.39	4.71	3.96 $\pm$ 0.03	4.46 $\pm$ 0.00
S <sub>R</sub>	0.94	1.00 $\pm$ 0.13	0.98 $\pm$ 0.17	0.74	1.20 $\pm$ 0.11	0.84 $\pm$ 0.04
S <sub>275-295</sub> (nm <sup>-1</sup> )	0.0129	0.014 $\pm$ 0.001	0.014 $\pm$ 0.001	0.013	0.014 $\pm$ 0.000	0.013 $\pm$ 0.000
S <sub>350-400</sub> (nm <sup>-1</sup> )	0.014	0.014	0.015	0.017	0.012	0.015
S <sub>300-700</sub> (nm <sup>-1</sup> )	0.011	0.014 $\pm$ 0.001	0.014 $\pm$ 0.001	0.016	0.012 $\pm$ 0.000	0.014 $\pm$ 0.000
a <sub>440</sub> (Napierian m <sup>-1</sup> )	5.89	7.77 $\pm$ 5.26	6.02 $\pm$ 2.48	2.35	10.60 $\pm$ 1.57	3.45 $\pm$ 0.04
SUVA <sub>254</sub> (decadic L mg <sup>-1</sup> m <sup>-1</sup> )	3.12	3.31 $\pm$ 0.98	3.34 $\pm$ 0.26	3.94	1.37 $\pm$ 0.10	2.52 $\pm$ 0.04
NO <sub>3</sub> <sup>-</sup> (mg-N L <sup>-1</sup> )	1.70	0.32 $\pm$ 0.22	0.33 $\pm$ 0.05	0.10	0.40 $\pm$ 0.14	1.37 $\pm$ 1.85
NH <sub>4</sub> <sup>+</sup> (mg-N L <sup>-1</sup> )	15.00 $\pm$ NA	11.00 $\pm$ 3.81	10.50 $\pm$ 5.45	1.00 $\pm$ NA	40.00 $\pm$ 1.41	0.00 $\pm$ 0.00
pH	7.89	7.82 $\pm$ 0.34	7.69 $\pm$ 0.64	8.03	7.81 $\pm$ 0.14	8.21 $\pm$ 0.14
conductivity (μS cm <sup>-1</sup> )	489.3	418.8 $\pm$ 38.32	404.2 $\pm$ 45.74	205.8	880.4 $\pm$ 0.42	620.37 $\pm$ 11.27
alkalinity (meq. L <sup>-1</sup> )	1.5	1.8 $\pm$ 0.2	1.6 $\pm$ 0.6	1.5	4.4 $\pm$ 0.3	2.0 $\pm$ 0.1
S <sub>AMX,DOM</sub>	0.93	0.90 $\pm$ 0.04	0.91 $\pm$ 0.02	0.95	0.88 $\pm$ 0.01	0.94 $\pm$ 0.00
S <sub>ATL,DOM</sub>	0.89	0.84 $\pm$ 0.06	0.86 $\pm$ 0.02	0.92	0.83 $\pm$ 0.01	0.91 $\pm$ 0.00
S <sub>EE2,DOM</sub>	0.86	0.79 $\pm$ 0.07	0.81 $\pm$ 0.03	0.89	0.77 $\pm$ 0.01	0.87 $\pm$ 0.00
DOM C18 retention peak area counts (approximate total)	1491743	606335 $\pm$ 216581	493417 $\pm$ 391199	37997	45564.5 $\pm$ 3244	129718 $\pm$ 152372

## Section S7: DOM polarity assessment

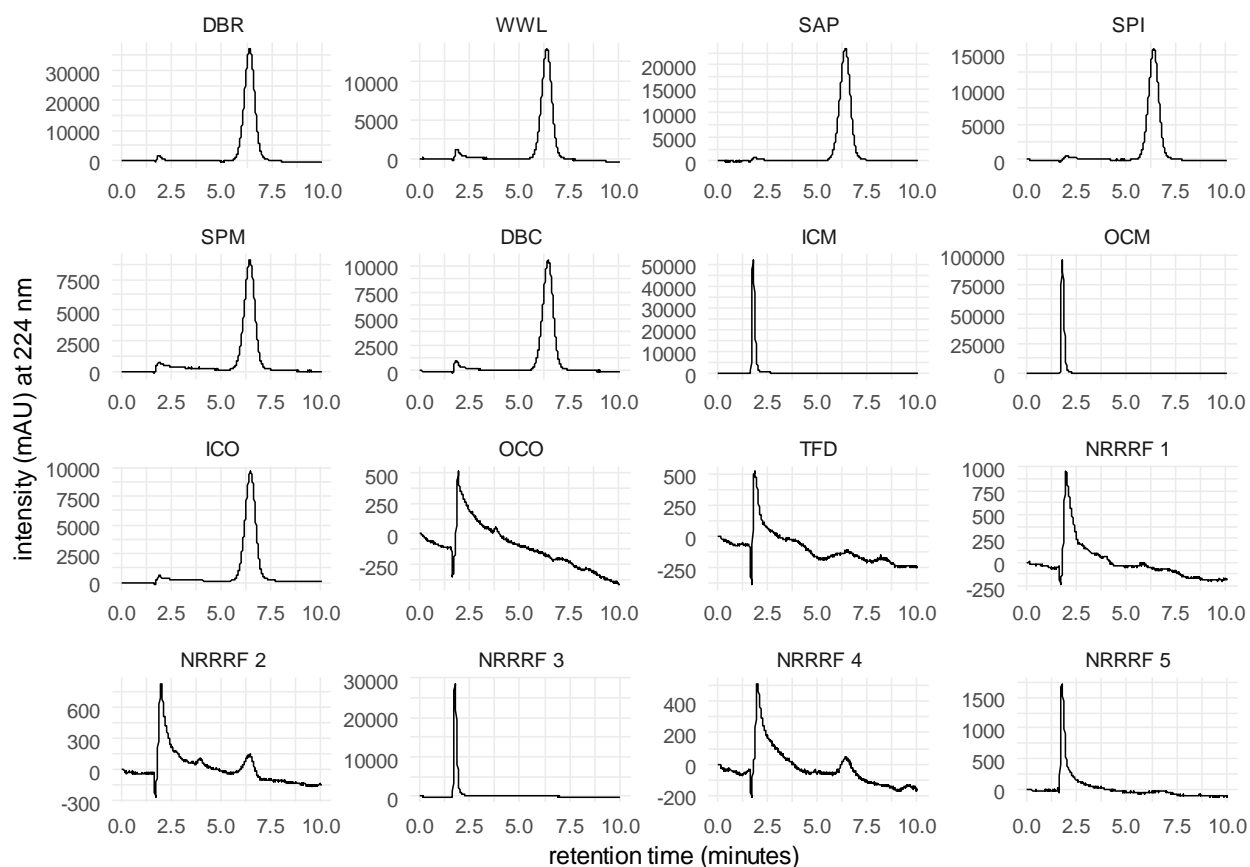


Figure S4: UV chromatogram for the different DOM samples collected from the two sampling sites. DOM elution represented at 224 nm. Samples are arranged in process sequence of the respective sites. DBR to TFD are samples from the treatment wetland site and NRRRF1 to NRRRF5 are from the wastewater treatment plant. Acronyms and process locations are described in Section S1. In comparison to the other wetland samples, OCO and TFD had substantially lower UV response. NRRRF 3 sample has 3.5 mg/L of nitrate which is the reason why it has a higher intensity reading compared to other NRRRF samples. Wetland site samples have negligible nitrate.

Table S6: List of hydrophilic DOM samples and hydrophobic DOM samples characterized in this study.

Hydrophilic DOM samples	ICM, OCM, OCO, TFD, NRRRF 1, NRRRF 2, NRRRF 3, NRRRF 4, and NRRRF 5
Hydrophobic DOM samples	DBR, WWL, SAP, SPI, SPM, DBC, and ICO

## Section S8: Photodegradation kinetics

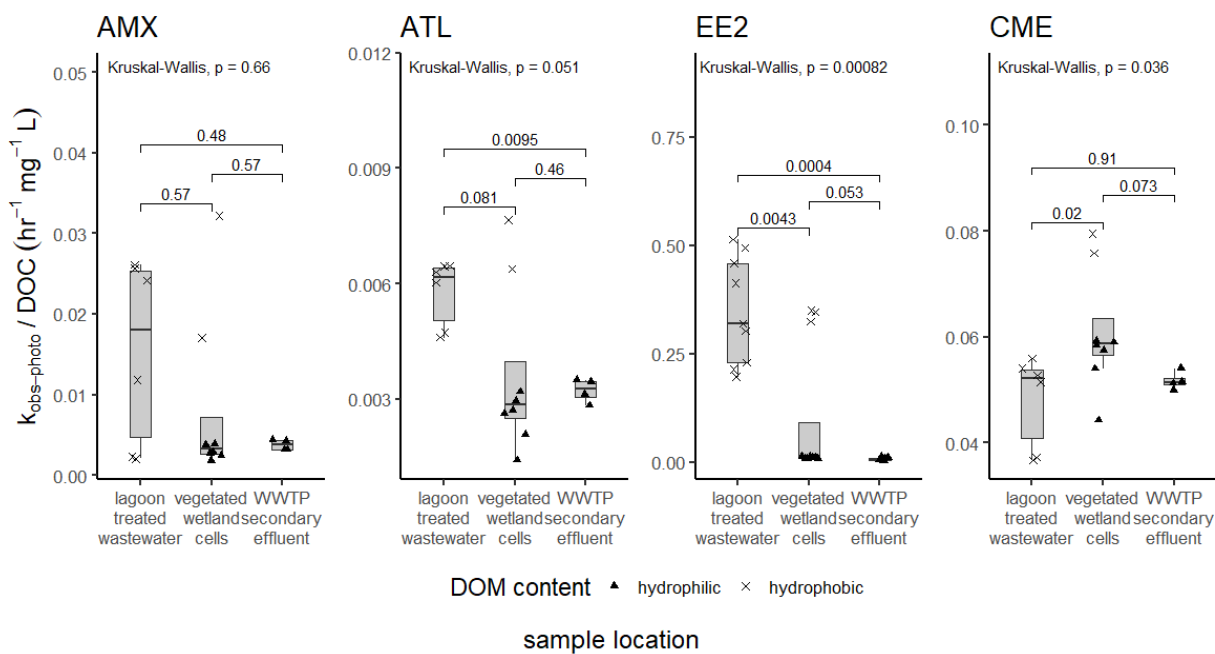


Figure S5: Carbon-normalized photodegradation rate constants for the target pharmaceuticals. Results are grouped for the different sampling locations. Symbol shapes indicate DOM polarity type. Each symbol represents a replicate from the irradiation experiments. There were three replicates for EE2 and two replicates for AMX, ATL, and CME. p-values for group wise comparisons and global p-values are also denoted.

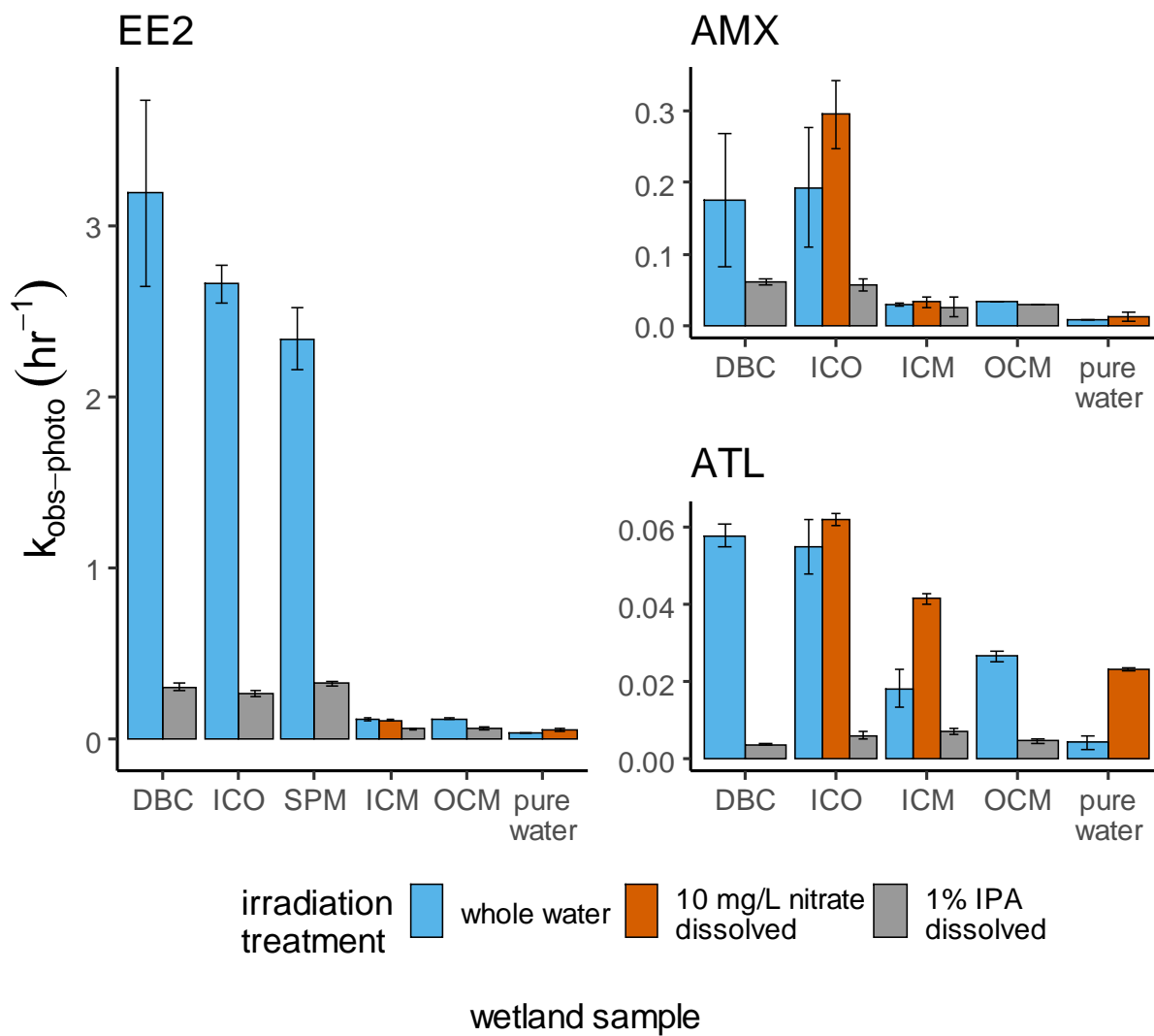


Figure S6: Photodegradation rate constants of target pharmaceuticals from experiments with dissolved nitrate and IPA.

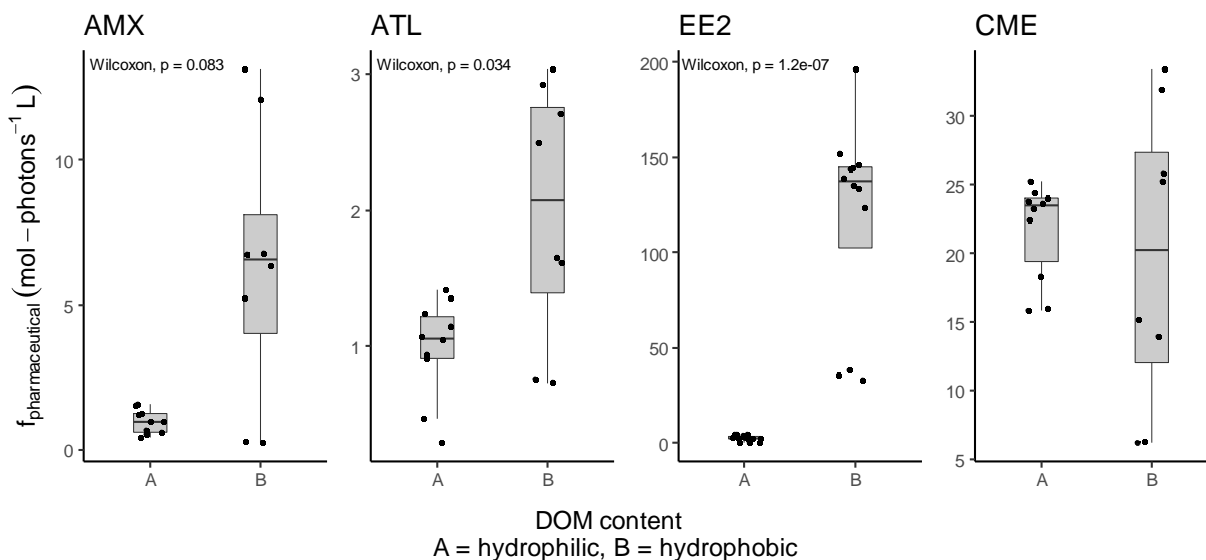


Figure S7: Quantum yield coefficients for indirect photodegradation of pharmaceuticals. Results grouped as per different DOM types. Each symbol represents a replicate from the irradiation experiments. There were three replicates for EE2 and two replicates for AMX, ATL, and CME. *p*-values for group wise comparisons are also denoted.

## Section S9: Steady state concentration estimates

Table S7: Steady state concentration of  $\cdot\text{OH}$  estimated using bi-molecular rate constants and quencher experiment results for selected samples.

wetland sample	DOM polarity type	$[\cdot\text{OH}]_{ss}$ (M) estimates based on quencher experiments with IPA		
		$\frac{k_{obs,photo-\cdot\text{OH},AMX}}{k_{AMX,\cdot\text{OH}}}$	$\frac{k_{obs,photo-\cdot\text{OH},ATL}}{k_{ATL,\cdot\text{OH}}}$	$\frac{k_{obs,photo-\cdot\text{OH},EE2}}{k_{EE2,\cdot\text{OH}}}$
ICO	hydrophobic	$(5.43 \pm 3.34) \times 10^{-15}$	$(1.81 \pm 0.26) \times 10^{-15}$	$(6.10 \pm 0.28) \times 10^{-14}$
DBC	hydrophobic	$(4.60 \pm 3.74) \times 10^{-15}$	$(2.00 \pm 0.10) \times 10^{-15}$	$(7.35 \pm 1.39) \times 10^{-14}$
ICM	hydrophilic	$(5.43 \pm 0.60) \times 10^{-16}$	$(4.05 \pm 1.83) \times 10^{-16}$	$(1.39 \pm 0.21) \times 10^{-15}$
OCM	hydrophilic	$(1.80 \pm 0.24) \times 10^{-16}$	$(8.12 \pm 0.52) \times 10^{-16}$	$(1.37 \pm 0.15) \times 10^{-15}$
SPM	hydrophobic	-	-	$(5.13 \pm 0.46) \times 10^{-14}$
10 mg-N L <sup>-1</sup> in pure water	-	$(4.59 \pm 2.59) \times 10^{-16}$	$(8.56 \pm 0.12) \times 10^{-16}$	$(1.27 \pm 0.23) \times 10^{-15}$

## Section S10: Amoxicillin degradation in the dark controls

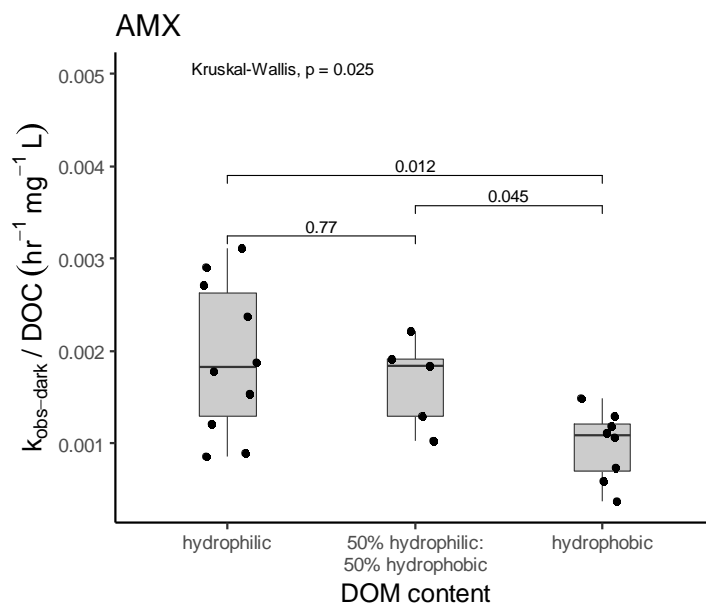


Figure S8: Carbon-normalized pseudo-first order rate constants for AMX degradation in the dark controls. Results grouped as per different DOM types. Each symbol represents a replicate from the irradiation experiments.  $p$ -values for group wise comparisons and global  $p$ -values are also denoted.

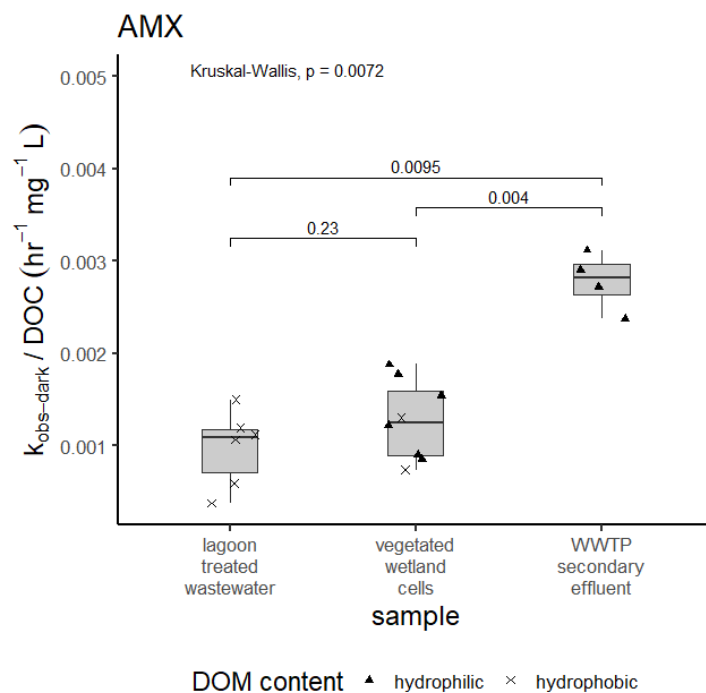


Figure S9: Carbon-normalized pseudo-first order rate constants for AMX degradation in the dark controls. Results grouped as per different sampling locations. Each symbol represents a replicate from the irradiation experiments. Symbol shapes indicate DOM type.

## Section S11: Noteworthy correlations

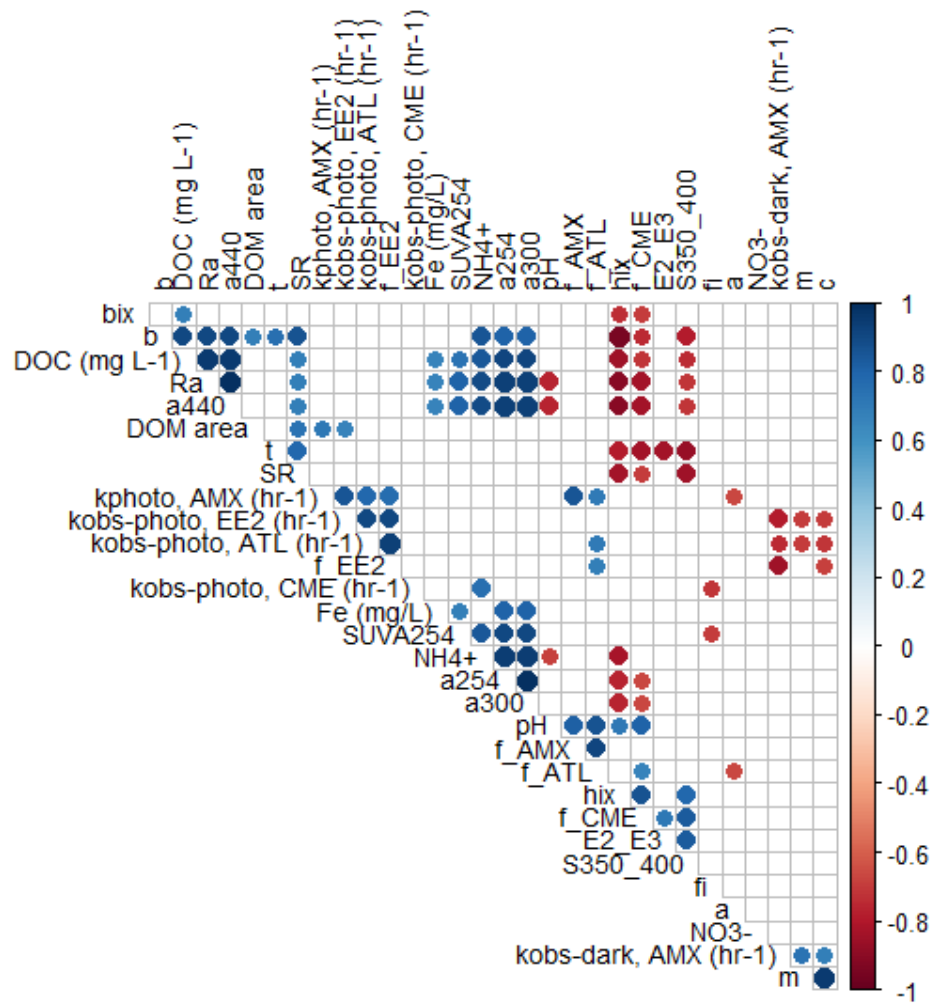


Figure S10: Correlation plot matrix shows the correlations between quantifiable DOM characteristics and photodegradation metrics. Statistically significant ( $p < 0.05$ ) correlations are displayed as colored circles. Blue circles represent positive correlations and negative correlations are shown in red. The color intensity and size of the circle is proportional to the correlation.

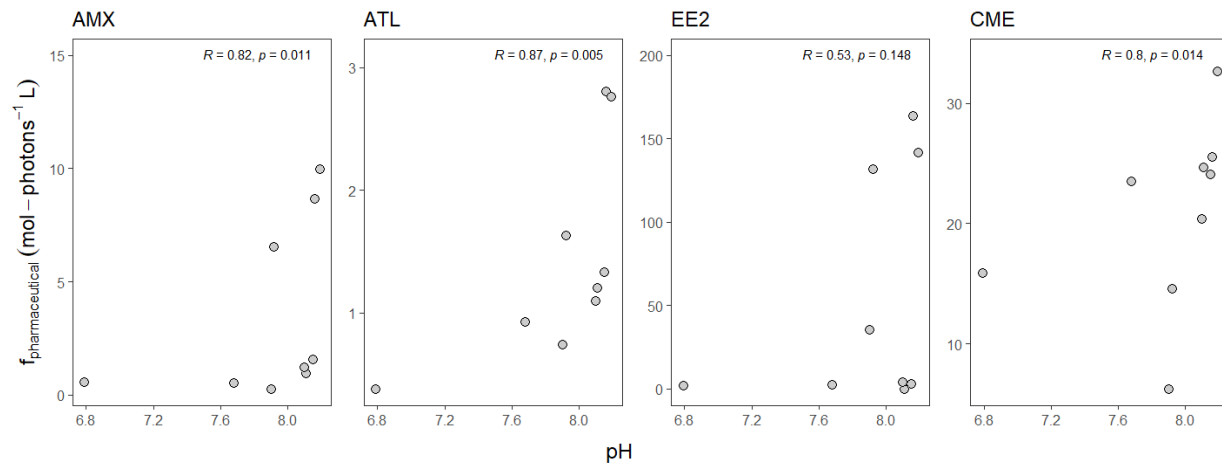


Figure S11: Scatter plots representing quantum yields coefficients for indirect photodegradation of pharmaceuticals ( $f_{\text{pharma.}}$ ) vs. pH.

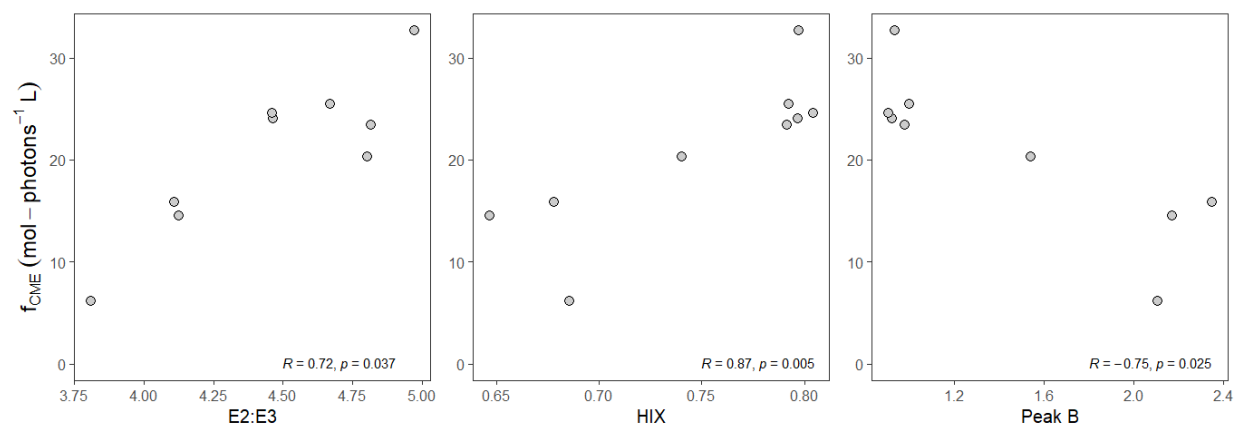


Figure S12: Scatter plots representing quantum yield coefficient of cimetidine indirect photodegradation ( $f_{\text{CME}}$ ) vs. selective optical indicators of DOM.

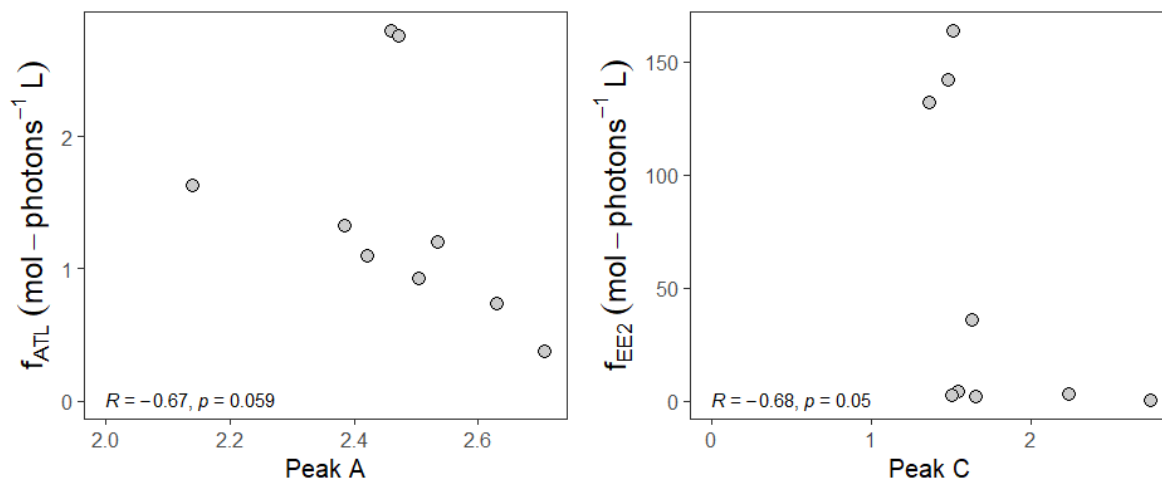


Figure S13: Scatter plots representing indirect photodegradation quantum yield coefficients of atenolol ( $f_{\text{ATL}}$ ) and 17 $\alpha$ -ethinylestradiol ( $f_{\text{EE2}}$ ) vs. EEM Peaks A and C, respectively.



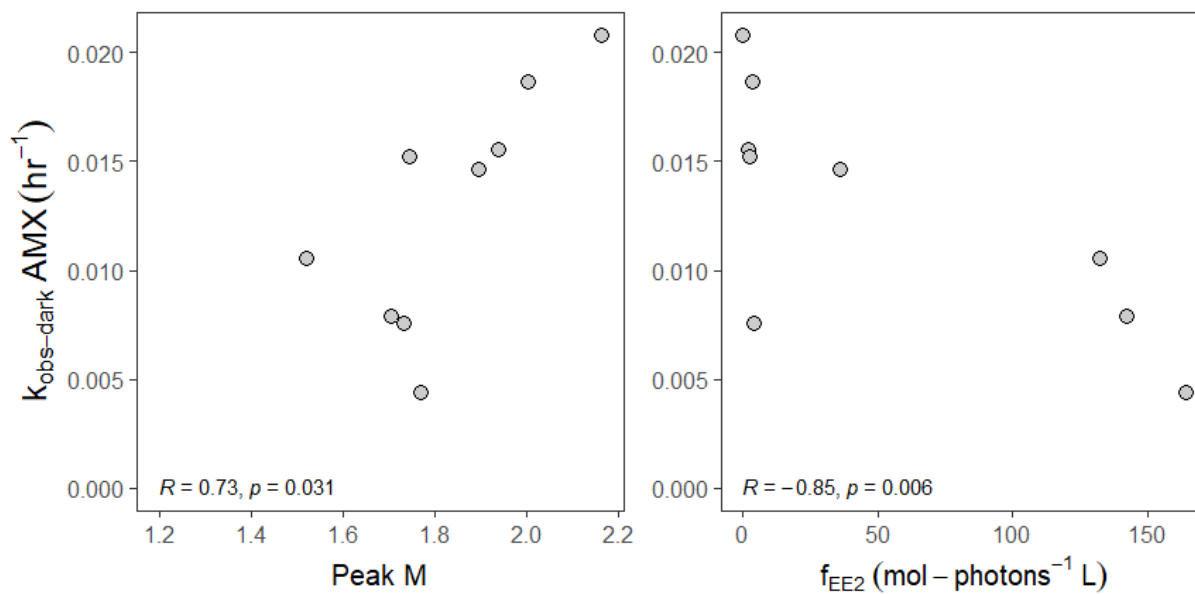


Figure S14: Scatter plots representing pseudo first-order degradation rate constants for the dark controls from AMX experiments vs EEM Peak M and indirect photodegradation quantum yield coefficient of 17 $\alpha$ -ethinylestradiol ( $f_{\text{EE2}}$ ).

## Section S12: References

- Andreozzi, R., Caprio, V., Ciniglia, C., De Champdoré, M., Lo Giudice, R., Marotta, R., Zuccato, E., 2004. Antibiotics in the environment: Occurrence in Italian STPs, fate, and preliminary assessment on algal toxicity of amoxicillin. *Environ. Sci. Technol.* 38, 6832–6838. <https://doi.org/10.1021/es049509a>
- Apell, J.N., McNeill, K., 2019. Updated and validated solar irradiance reference spectra for estimating environmental photodegradation rates. *Environ. Sci. Process. Impacts* 21, 427–437. <https://doi.org/10.1039/C8EM00478A>
- Benner, J., Salhi, E., Ternes, T., von Gunten, U., 2008. Ozonation of reverse osmosis concentrate: Kinetics and efficiency of beta blocker oxidation. *Water Res.* <https://doi.org/10.1016/j.watres.2008.04.002>
- Cass, Q.B., Gomes, R.F., Calafatti, S.A., Pedrazzoli, J., 2003. Determination of amoxicillin in human plasma by direct injection and coupled-column high-performance liquid chromatography, in: *Journal of Chromatography A*. [https://doi.org/10.1016/S0021-9673\(02\)01660-6](https://doi.org/10.1016/S0021-9673(02)01660-6)
- Ekrem Karpuzcu, M., McCabe, A.J., Arnold, W.A., 2016. Phototransformation of pesticides in prairie potholes: effect of dissolved organic matter in triplet-induced oxidation. *Environ. Sci. Process. Impacts* 18, 237–245. <https://doi.org/10.1039/C5EM00374A>
- Huber, M.M., Canonica, S., Park, G.-Y., von Gunten, U., 2003. Oxidation of pharmaceuticals during ozonation and advanced oxidation processes. *Environ. Sci. Technol.* 37, 1016–24. <https://doi.org/10.1021/es025896h>
- Jasper, J.T., Sedlak, D.L., 2013. Phototransformation of Wastewater-Derived Trace Organic Contaminants in Open-Water Unit Process Treatment Wetlands. *Environ. Sci. Technol.* 47, 10781–10790. <https://doi.org/10.1021/es304334w>
- Küster, A., Alder, A.C., Escher, B., Duis, K., Fenner, K., Garric, J., Hutchinson, T., Lapen, D., Péry, A., Römbke, J., Snape, J., Ternes, T., Topp, E., Wehrhan, A., Knacker, T., 2007. Environmental Risk Assessment of Human Pharmaceuticals in the European Union - A Case Study with the  $\beta$ -blocker Atenolol. *Integr. Environ. Assess. Manag.* preprint, 1. [https://doi.org/10.1897/IEAM\\_2009-050.1](https://doi.org/10.1897/IEAM_2009-050.1)
- Langlois, M.C., Weavers, L.K., Chin, Y.-P., 2014. Contaminant-mediated photobleaching of wetland chromophoric dissolved organic matter. *Environ. Sci. Process. Impacts* 16, 2098. <https://doi.org/10.1039/C4EM00138A>
- Latch, D.E., Stender, B.L., Packer, J.L., Arnold, W.A., McNeill, K., 2003. Photochemical Fate of Pharmaceuticals in the Environment: Cimetidine and Ranitidine. *Environ. Sci. Technol.* 37, 3342–3350. <https://doi.org/10.1021/es0340782>
- Liu, Q.-T., Williams, H.E., 2007. Kinetics and Degradation Products for Direct Photolysis of  $\beta$ -Blockers in Water. *Environ. Sci. Technol.* 41, 803–810. <https://doi.org/10.1021/es0616130>
- Ren, D., Huang, B., Bi, T., Xiong, D., Pan, X., 2016. Effects of pH and dissolved oxygen on the photodegradation of 17 $\alpha$ -ethynylestradiol in dissolved humic acid solution. *Environ. Sci. Process. Impacts* 18, 78–86. <https://doi.org/10.1039/C5EM00502G>
- Song, W., Chen, W., Cooper, W.J., Greaves, J., Miller, G.E., 2008a. Free-Radical Destruction of  $\beta$ -Lactam Antibiotics in Aqueous Solution. *J. Phys. Chem. A* 112, 7411–7417. <https://doi.org/10.1021/jp803229a>
- Song, W., Cooper, W.J., Mezyk, S.P., Greaves, J., Peake, B.M., 2008b. Free Radical Destruction of  $\beta$ -

- Blockers in Aqueous Solution. *Environ. Sci. Technol.* 42, 1256–1261.  
<https://doi.org/10.1021/es702245n>
- Wang, L., Xu, H., Cooper, W.J., Song, W., 2012. Photochemical fate of beta-blockers in NOM enriched waters. *Sci. Total Environ.* 426, 289–95. <https://doi.org/10.1016/j.scitotenv.2012.03.031>
- Xu, H., Cooper, W.J., Jung, J., Song, W., 2011. Photosensitized degradation of amoxicillin in natural organic matter isolate solutions. *Water Res.* 45, 632–8. <https://doi.org/10.1016/j.watres.2010.08.024>
- Yamamoto, H., Nakamura, Yudai, Moriguchi, S., Nakamura, Yuki, Honda, Y., Tamura, I., Hirata, Y., Hayashi, A., Sekizawa, J., 2009. Persistence and partitioning of eight selected pharmaceuticals in the aquatic environment: Laboratory photolysis, biodegradation, and sorption experiments. *Water Res.* 43, 351–362. <https://doi.org/10.1016/j.watres.2008.10.039>
- Yoon, K.H., Lee, S.Y., Kim, W., Park, J.S., Kim, H.J., 2004. Simultaneous determination of amoxicillin and clavulanic acid in human plasma by HPLC-ESI mass spectrometry. *J. Chromatogr. B Anal. Technol. Biomed. Life Sci.* <https://doi.org/10.1016/j.jchromb.2004.09.018>
- Zenobio, J.E., Sanchez, B.C., Leet, J.K., Archuleta, L.C., Sepúlveda, M.S., 2015. Presence and effects of pharmaceutical and personal care products on the Baca National Wildlife Refuge, Colorado. *Chemosphere.* <https://doi.org/10.1016/j.chemosphere.2014.10.050>